NASA Technical Memorandum 84311

Optimal Feedback Strategies for Pursuit-Evasion and Interception in a Plane

N. Rajan and M. D. Ardema

February 1983

NASA
National Aeronautics and
Space Administration

NASA Technical Memorandum 84311

Optimal Feedback Strategies for Pursuit-Evasion and Interception in a Plane

N. Rajan
M. D. Ardema, Ames Research Center, Moffett Field, California

National Aeronautics and
Space Administration

Ames Research Center
Moffett Field, California 94035

OPTIMAL FEEDBACK STRATEGIES FOR PURSUIT-EVASION AND INTERCEPTION IN A PLANE

N. Rajan* and M. D. Ardema

Ames Research Center

SUMMARY

Variable-speed pursuit-evasion and interception for two aircraft moving in a horizontal plane are analyzed in terms of a coordinate frame fixed in the plane at termination. Each participant's optimal motion can be represented by extremal trajectory maps. These maps are used to discuss suboptimal approximations that are independent of the other participant. A method of constructing sections of the Barrier, Dispersal, and control-level surfaces and thus determining feedback strategies is described. Some examples are shown for pursuit-evasion and the minimum-time interception of a straight-flying target.

INTRODUCTION

The problems of aircraft pursuit-evasion and interception are complex because the aircraft dynamics are nonlinear and of high dimension. Pursuit-evasion in a horizontal plane has five state variables and two control variables per aircraft. It is presently impossible to derive a feedback solution in a closed form for this problem. However, a feedback solution is essential for onboard flightpath management. Hence, in the past, three classes of methods for determining feedback strategies for pursuit-evasion have been explored.

The first class consists of methods that rely on computational techniques (refs. 1, 2) to solve the two-point boundary-value problem of determining the optimal controls from a given initial state. The techniques have then been combined with a discretization of the state-space to yield a "near-optimal" feedback solution to pursuit-evasion. To keep the computational effort at a practical level for a flight computer, the aircraft models utilized in the above studies have been relatively simple. Also, a fixed-time terminal miss-distance formulation of pursuit-evasion was used to obviate difficulties with singular surfaces (ref. 3).

A recent study (ref. 4) which can be considered to fall in the first category of methods, employs parameter optimization to determine optimal evasive strategies against a pursuer flying pure pursuit. The duration of the engagement is left open; it is one of the parameters of the optimization problem. The aircraft are modeled as point-masses moving in three dimensions with realistic lift, drag, and thrust functions. This work is limited by the assumption regarding the pursuer's behavior and by the fact that a large amount of computation is required to determine the optimal controls from a single initial state.

In the second class of methods, an attempt is made to obtain an approximate closed-form feedback solution. Forced singular-perturbation techniques (refs. 5-8) use the time-scale separation inherent in some aircraft maneuvers to reduce the order of the problem and to obtain an analytical solution. The latter serves as an approximate guidance law that can be readily implemented on board. These methods are limited by the assumptions made in separating the time scales. The domain of validity of the solution can be determined by comparison with exact solutions.

The third class of methods for the interception/pursuit-evasion problem proceeds by flooding the state-space with extremals. Since the terminal manifold has a

---

*NRC Research Associate.

dimension of four, finding the extremal that passes through a given initial state requires a large amount of computation. However, since for a feedback solution the optimal controls have to be determined all over the state-space, flooding provides a feasible solution. Also, the computational effort can be reduced by assuming that all the extremals are of sufficiently long duration to permit the aircraft to accelerate to maximum speed. If this assumption is made, all trajectories include cruise arcs that are straight dashes flown at the upper speed limit. The extremals are then a one-parameter family and the initial conditions can be matched through a one-dimensional search. The study of turns to a line or a point reported in reference 9 is based upon the assumption of a cruise arc. In this paper, it is not assumed that all extremals include cruise arcs.

For interception and pursuit-evasion, the construction of a feedback solution by flooding is complicated by singular surfaces, such as Barrier and Dispersal surfaces. In situations in which the evader can escape from the pursuer for some initial conditions, the Barrier bounds the region of the state-space in which the evader can be captured. Where the evader/target can be captured regardless of the initial condition, the Barrier is an open surface across which the time-to-capture is discontinuous. Along a Universal (ref. 3) surface, one aircraft employs a singular control. On a Dispersal surface, the gradient of the time-to-capture is discontinuous. At a point on a Dispersal surface, one aircraft can choose between two distinct strategies and still get the same payoff. These surfaces are an inherent part of the feedback solution.

Barrier sections for variable-speed pursuit-evasion in a plane were reported in references 10-13. The analysis proceeded by describing the game in a coordinate system fixed in the plane, with the origin at the pursuer's final position at capture and the x-axis along the terminal line of sight (LOS). This led to a decoupling of the equations into two disparate sets, one for each aircraft. By giving different values to the terminal-velocity vector, a map of extremals is generated for each aircraft independent of the other. This extremal trajectory map (ETM) can then be used to study any planar encounters in which the given aircraft participates. A method of computing Barrier cross sections by directly iterating on the aircraft's terminal speeds to match the given initial speeds and relative heading was developed, and example cross sections were presented for the case in which both aircraft had the same capability but the pursuer had an initial turn-rate advantage. The above analysis was applied to minimum-time interception in the horizontal plane in reference 14 where a method of locating Barrier and Dispersal points by drawing isochrone (constant minimum-time-locus) sections was developed.

The previous studies in pursuit-evasion concentrated on solving the game of kind (ref. 3), which consists of determining the regions of the state-space from which the evader can be captured. The game of degree (ref. 3), which describes the strategies within the capture region, was not studied. The work on interception (ref. 14) examined sections of the Barrier and Dispersal surfaces; control-level surfaces were not studied.

In this paper, the ETM idea is explored further, especially in terms of its potential as a tool for developing approximations to the optimal interception strategy. The ETMs are drawn for given times-to-go and initial speeds. The construction of a feedback solution for pursuit-evasion and interception by drawing isochrone sections is explained. Example sections and trajectories in the plane are presented. Extremal trajectory maps are examined in the next section, as well as a discussion of cruise arcs. The synthesis of a feedback solution from ETMs is described and examples are given in the third section.

EXTREMAL TRAJECTORY MAPS

Definition

In references 10-14, the equations of motion for pursuit-evasion and minimum-time interception are written in a system of coordinates that has its origin fixed at the pursuer/interceptor's terminal position and has its x-axis along the terminal line of sight (fig. 1). For the backward integration of extremals, this decouples the pursuer/interceptor's motion from that of the evader/target. Each set of extremals is a family characterized by all possible values of the corresponding terminal-velocity vector. The family is generated by integrating the equations ($\circ \equiv d/d\tau$, where $\tau = t_f - t$)

$$\overset{\circ}{x} = -M \cos \beta \tag{1}$$

$$\overset{\circ}{y} = -M \sin \beta \tag{2}$$

$$\overset{\circ}{\beta} = -f(M)\omega \tag{3}$$

$$\overset{\circ}{M} = B(M) + C(M)\omega^2 - A(M)\pi \tag{4}$$

$$\overset{\circ}{p}_M = -\cos \beta - (p_M + \bar{\mu})d\overset{\circ}{M}/dM - y\, d\overset{\circ}{\beta}/dM \tag{5}$$

subject to the initial conditions (at $t = t_f$)

$$x = y = p_M = 0 \tag{6}$$

$$\beta = \beta_f , \qquad M = M_f \tag{7}$$

In these equations, the heading β is measured relative to the x-axis, M is the Mach number, p_M is a normalized speed adjoint, and $\bar{\mu}$ is a Kuhn-Tucker multiplier accounting for the constraint on the Mach number $M \in [\underline{M},\bar{M}]$, where $\underline{M}$ is the stall speed at zero bank angle and $\bar{M}$ is the maximum velocity placard limit (ref. 9). The throttle setting π and the bank control ω are chosen such that $\pi \in [0,1]$ and $\omega \in [-1,1]$.

The description of aircraft motion in equations (1)-(4) is the same as that given in reference 10. The functions f, B, C, and A represent the maximum instantaneous turn rate, the zero-bank drag, the lift-induced drag at maximum bank, and the maximum thrust. The interception/pursuit-evasion problem is formulated with time-to-capture as payoff, with capture occurring when the terminal line-of-sight separation between the aircraft equals a constant R (fig. 1) and is shrinking.

In reference 10, where the ETM idea was first derived, it is shown that the optimal controls π and ω in equations (1)-(5) are given by the expressions

$$\left.\begin{aligned} \pi &= 1 \\ \omega &= \text{sat}\{-fy/[2C(p_M + \bar{\mu})]\} \end{aligned}\right\} \quad \text{for} \quad p_M + \bar{\mu} < 0 \tag{8}$$

$$\left.\begin{aligned} \pi &= 0 \\ \omega &= \text{sgn}(y) \end{aligned}\right\} \quad \text{for} \quad p_M + \bar{\mu} > 0 \tag{9}$$

An extremal trajectory map consists of extremals satisfying equations (1)-(5) integrated backward in time for a fixed time-to-go τ_f. The terminal heading β_f is the parameter characterizing the extremals. For each β_f value, the value of M_f is searched iteratively until the Mach number at $\tau = t_f$ equals a specified value M_o. The coordinates (x_o, y_o), the heading β_o, and the strategies (π, ω) are noted and stored. Although extremals can be integrated backward from the origin for all values of β_f between 0° and 180°, in practice, the extremals for which β_o is much more than 180° are generally not globally optimal (discussed in the following section), because there is usually a lower cost extremal passing through the given initial state.

Given the ETMs of the pursuing and evading aircraft, each pair of extremals (one from each map) can be put together to yield a candidate minimax optimal trajectory for the pursuit-evasion encounter (fig. 2). If the relative velocity component along the terminal LOS is negative, that is, if

$$M_{p_f} \cos \beta_{p_f} - M_{e_f} \cos \beta_{e_f} < 0 \tag{10}$$

((M_{p_f}, β_{p_f}) and (M_{e_f}, β_{e_f}) are the terminal-velocity vectors of the pursuer and evader, respectively) and if the extremal does not cross any singular surface (ref. 3) of the game (the following section, Feedback Solution), then the extremal is globally optimal. All the extremals that an aircraft may follow in any encounter are included in the ETM. The ETM is thus a good framework within which to study the optimal behavior of a given aircraft model and to explore suboptimal approximations to the extremal.

General Features

From the necessary conditions and as a result of experience with numerous examples, the general behavior of the extremals with variation in β_f can be deduced. It is determined that they are symmetric with respect to the x-axis for positive and negative values of β_f; positive values involve banking to the right and vice versa. For $\beta_f = 0°$, the extremal is full-throttle, level flight along the negative x-axis. For β_f values below β_ℓ, defined as

$$\beta_\ell \triangleq \tan^{-1}(2C/fM) \tag{11}$$

the bank control ω starts out partial and increases in retrograde time to unit magnitude. From equation (8), all partial-bank arcs are flown with full throttle. Once ω saturates, the throttle may later be switched to zero if the Mach number is above $\hat{M}$ (Mach number corresponding to the corner velocity (ref. 9); at $\hat{M}$, the load factor and lift limitations on the normal acceleration are equal). When β_f increases beyond β_ℓ, the extremals emanate from the origin with full bank. All full-bank segments of the extremals are generated using trajectory templates (ref. 10) (precomputed and stored long-duration trajectories flown at full bank). For $\beta_f > 90°$, the terminal controls are full-bank and zero throttle. In between $\beta_f = 90°$ and 100°, the throttle may be switched to 1 and back to 0 in retrograde time. If an extremal intersects the x-axis with $p_M > 0$, from equation (9) ω changes sign (fig. 3(a)). If, however, $p_M < 0$ as the extremal approaches the x-axis (fig. 3(b)), then equation (8) holds and ω changes gradually from +1 to -1 (or vice versa) over the intersection. The latter occurs if $M_f < \hat{M}$.

Since the Hamiltonian is linear in the throttle setting π, intermediate values of π are singular controls. For the aircraft model (ref. 9) used in this

investigation (an F-4C), partial thrust and zero bank are optimal only at the upper speed bound (ref. 10). Partial-thrust and full-bank singular arcs were not encountered in the computations.

Extremals and Approximations

A typical map of intermediate-duration extremals is shown in figures 4(a)-4(d) for the F-4C aircraft, flying at an altitude of 6.1 km. In all cases, the change in heading over the last 25 sec of flight is less than 6° (fig. 4(a)) and the bank control increases from about -0.1° to near zero (fig. 4(b)). The extremals can thus be described as consisting of a turning phase followed by an accelerating phase. During the first phase, the aircraft changes to the required heading, decelerating in the process (fig. 4(c)). Then in the second phase, the aircraft accelerates to the speed required for capture. In this particular family, both phases are of about equal duration, but as the time-to-go increases, turning occupies a smaller percentage of the time and vice versa. For large values of τ_f, the turning phase can be considered as a boundary layer, and singular perturbation approaches (refs. 5-7) can be successfully applied.

At the start of a turn, the throttle may be zero; however, it is switched to full a few seconds into the turn. For this aircraft example, on extremals that last 20 sec or more, zero-throttle segments take up relatively small portions of the flight time and can be safely ignored. The Mach number variation (fig. 4(c)) over the full-bank segments is less than 0.1; in this speed range the turn rate is inversely proportional to the Mach number and changes by less than 10%. Since full-bank segments are read off trajectory templates, they require very little computation time.

The acceleration phase consists of essentially straight flight at full throttle. The Mach number increment varies from 0.188 over 50 sec for $\beta_f = 0°$ to 0.236 over 35 sec for $\beta_f = 0.003°$. The difference in acceleration is due to the increase in drag at supersonic Mach numbers. The acceleration phase could be approximated by flight along a straight line that makes a small angle with the final LOS.

The possibility of approximating intermediate-duration extremals by separating them into turning and acceleration phases can be further explored by looking at extremals with the same initial speeds and turn angles but different duration. In figure 5 an extremal lasting 50 sec is compared with two others generated for 20 sec. In 20 sec, the turn angle for the long-duration extremal is 142° and the Mach number is 0.952. The other two extremals are chosen such that one ($\beta_f = 0.6°$) matches the Mach number and the other ($\beta_f = 0.7°$) the turn angle of the original extremal. The endpoints of these extremals are close to the 20-sec point of the original extremal.

For the remaining 30 sec, the flightpath is almost straight. If extremals that consist mainly of turning flight are approximated closely, the suboptimal approximations to extremals of longer duration are simply the short-duration approximations plus straight flight. The full-bank segments of turning extremals are read off templates. The partial-bank segments can be approximated by a number of fixed-bank segments (fig. 6) which can also be generated using templates.

The above example also suggests that beyond a duration of 20 sec, an error in the initial guess of the duration of the encounter is not crucial. Given the initial speeds and relative heading of the vehicles in an encounter, an estimate of the time-to-capture is the first step in generating the optimal flightpaths. This can be determined by inspecting plots of the turn angle, Mach number increment, and distance

covered against the time-to-go. Example plots for an initial Mach number of 0.9 are shown in figures 7(a)-7(c). In these figures, straight-flight extremals have their starting points on the zero-bank curve, those starting with $\omega = 0.5$ in magnitude fall on the half-bank curve, and those starting with ω just saturated fall on the bank-saturation curve. Thus, in between the zero bank and half-bank curves, lie all the extremals with the initial ω between 0 and 0.5; between half-bank and bank saturation, lie all extremals with ω initially between 0.5 and 1.0; and outside the bank-saturation curve lie all the extremals that have a finite-duration initial full-bank arc. The values of β_f at the different times-to-go for figure 7 are shown in table 1.

For larger values of β_f than those shown in table 1, the entire extremal is flown at full bank. The characteristics of such extremals are given in table 2. The turn angles for these would be above the bank-saturation curve in figure 7(a); the Mach number increment and distance traversed would be below the bank-saturation curves in figures 7(b) and 7(c). From the table, the turn angle for the 15-sec extremal is 166° and it is greater than 200° for the 20-sec extremal. For capture times greater than 20 sec, the above extremals are not globally optimal because they fall beyond Dispersal points (ref. 14).

Thus, the vast majority of the extremals that appear in planar encounters have both full-bank and partial-bank segments. For extremals with the same capture times, an increase in the duration of the full-bank arc means an increase in the turn angle but reductions in the Mach number increment and distance traversed. The turn angles of extremals with full-bank arcs will be above the bank-saturation curve in figure 7(a); their Mach number increment and distance traversed will be below it in figures 7(b) and 7(c). Thus, if the turn angle is to be about 60° and the distance to be traversed by the aircraft about 6 km, the time-to-go must be at least 20 sec (fig. 7(c)). The condition on the terminal velocities at capture, equation (10), gives a lower bound on the acceleration to be achieved. For extremals of duration greater than 20 sec, termination is usually a tail-chase, with β_{p_f} and $\beta_{e_f} \approx 0°$, making equation (10) a condition on the terminal speeds M_{p_f} and M_{e_f}. If a nonevading target flying in a straight line at Mach 1.0 is to be intercepted, the interceptor's turn angle equals the target's initial heading relative to it, and its Mach number increment must be at least 0.1 (initial interceptor Mach number = 0.9). Starting from the lower bound on capture time that meets the requirement on the turn angle and speed increment, the capture time is increased until the extremal that satisfies the initial conditions and leads to capture of the target is found.

As the duration of the extremal increases, the terminal heading β_f tends to zero and the terminal Mach number M_f increases towards $\bar{M}$. Once M_f reaches $\bar{M}$, the extremals consist of an initial accelerating turn, a very short circular arc at constant speed $\bar{M}$, and a straight dash at $\bar{M}$ (fig. 8(a)). The circular arc and the straight dash are together called a cruise arc (ref. 9). Extremals that end in cruise arcs are characterized by a single parameter, the heading β_s (fig. 8(a)). Thus, matching the initial conditions can be done by a one-parameter search. Typically, the turn angle and initial speed are matched. Then the length of the straight dash is adjusted to match the initial position. The development of necessary conditions for cruise arcs is detailed in reference 9. The only difference is that for an interception, there is no requirement for a final turn from the cruise arc, as there is for turns to a line or point with specified final heading. An example trajectory is shown in figure 8(b); the interceptor's initial Mach number is 1.3 and the flight direction is 150 sec. The duration of the circular segment is extremely short, and is closely approximated by a spike in heading of about 10^{-8} deg. In retrograde time,

the unconstrained arc in such an extremal starts with $M = \bar{M}$, decelerates to some Mach number below $\bar{M}$, and then once again accelerates to $\bar{M}$. The intermediate Mach number decreases with a decrease in the magnitude of β_s; however, for $\beta_s < 10^{-8}$ deg, there is a loss of significance in the computation. This is overcome in reference 9 by computing the heading and Mach number on the unconstrained arc 1 sec away from the junction, approximately. Since the turning phase in these extremals occupies a small percentage of the time, they can as well be approximated by a full-bank turn and a straight dash (refs. 10, 13).

THE FEEDBACK SOLUTION

Taken together, the extremal trajectory maps of the two aircraft taking part in an encounter contain all the possible optimal paths in the plane. However, any given pair of extremals, taken one from each map, need not lead to a globally optimal saddle-point encounter. Firstly, the reachability condition on the relative velocity at termination, equation (10), may not be met for the assumed value of the time-to-go τ_f, the initial state is then beyond the Barrier. Secondly, the initial state may lie on the wrong side of a Dispersal surface so that there are extremals of shorter duration passing through it. The location of Barrier and Dispersal points is hence an inherent part of the solution; those locations have been discussed in reference 14.

Once the Barrier and Dispersal points are determined, the control strategies have to be mapped for the different regions of the state-space. Since the state-space dimension is four or five, the mapping of strategies is presented by sectioning: cross sections are taken with the initial interceptor/pursuer and target/evader speeds and relative heading held constant. The sections are then plotted relative to the interceptor/pursuer and become curves in the plane of the encounter. Within each section, the controls are mapped by drawing sections of the isochrones (constant-time-to-go loci). On each isochrone section, the points where the initial bank control ω is zero, half (half-bank point), or just saturates (bank-saturation point) are marked. The curves linking such points on the isochrone sections for different times-to-go are sections of the bank-level surfaces. The bank strategy changes across these surfaces. The construction of isochrones leads to the mapping of Dispersal, Barrier, and control-level surface sections. The construction of isochrones for planar pursuit-evasion and interception is discussed next.

Construction of Isochrones

Assume that the pursuer and evader ETMs are as shown in figures 9(a) and 9(b), respectively. Each map consists of extremals generated for the same time-to-go, with the terminal headings β_{p_f} (β_{e_f}) as a parameter. For each extremal, the initial Mach number is M_{p_o} (M_{e_o}) and the initial heading measured relative to the terminal line of sight equals β_{p_o} (β_{e_o}). The isochrone section being constructed has M_{p_o}, M_{e_o}, and β_o specified, where β_o is the initial relative heading

$$\beta_o = \beta_{p_o} - \beta_{e_o} \tag{12}$$

For any given pair of terminal headings β_{p_f}, β_{e_f}, the terminal Mach numbers M_{p_f} and M_{e_f} have already been iterated to match the starting Mach numbers M_{p_o}, M_{e_o}.

For matching the relative heading, β_{p_f} is taken as a fixed parameter and β_{e_f} is determined by searching in the evader's ETM. In the construction of a point on the isochrone, figure 9(c), the pursuer's extremal is first laid off as PA. The terminal LOS is AB. Since the evader's terminal heading has been determined, its extremal can be laid off as shown, EB. The point E is the point on the locus, provided the terminal LOS rate is negative; that is, equation (10) is satisfied.

Different values of β_{p_f} give other points on the isochrone section. The values of β_{p_f} are selected such that all significant points on the section are mapped. These include the zero-, half-, and full-bank points (the bank at start is zero, half, and full, respectively), as well as any points where the bank angle or throttle switch. For any given section, some of the above points may not appear, either because the reachability condition is not satisfied or because they fall beyond a Dispersal point. All these points depend on only one aircraft's terminal heading, either β_{p_f} or β_{e_f}. Once marked in an ETM, mapping them on any isochrone section requires only a search of the other aircraft's ETM. A Dispersal point occurs if, for either of the aircraft, two extremals with different values of the terminal heading pass through the same point in reduced space.

In interception, the target's motion is known in advance. Only the orientation of its terminal-velocity vector relative to the terminal line of sight changes in the selected coordinate system. Therefore, the target's ETM consists of the same path rotated through different terminal headings. For any given value of τ_f, the target's turn angle $\Delta\beta$ is constant, independent of the terminal heading. The latter is computed such that equation (12) is met for the β_o value specified for the section. Unlike the pursuit-evasion problem, searching of the other aircraft's ETM is unnecessary.

Examples

An isochrone section for pursuit-evasion is shown in figure 10. The initial speeds of the pursuer and evader are Mach 1.2 and 0.9, respectively. The same aircraft model is used for both players. The capture radius is 316 m, a typical value for an engagement in which the pursuer uses only guns. The section is drawn for a time-to-go of 50 sec and an initial relative heading of 180°. The encounter at D is depicted in the plane in figure 11. The sections for $\beta_o = \pm 180°$ intersect at D, which is a Dispersal point because the evader can choose to turn left or right and still be captured in the same time. The aircraft trajectories from the starting points C_1, C, C_2, and B on the $\beta_o = 180°$ section of figure 10 are shown in figures 12(a)-12(d). Figures 13(a)-13(c) show the variation of Mach number, heading, and bank control with time-to-go along the extremals flown from the points D to B. The values of the terminal-velocity vectors are given in table 3.

At D, the pursuer's initial bank angle is half its maximal value. The pursuer gradually levels out, turning 31.5° (figs. 11, 13) to align itself with the evader's anticipated heading and accelerates to Mach 1.377. The evader banks fully for 7.45 sec, then reduces bank angle and accelerates to Mach 1.184. In the first 8 sec it turns through 90°; its total turn angle over the 50 sec of flight is 148.5°. Of all the points on the isochrone section this is the farthest from the pursuer because the latter has to turn relatively little and can employ his speed advantage to cover more ground than the evader.

From D to B, the pursuer's turn angle increases, and its terminal Mach number and distance traversed fall; the reverse is true for the evader. At C (fig. 12(b)), the pursuer banks fully to the left for 7 sec and then gradually straightens out; its bank value falls below 0.1 after 20 sec of flight. Out of the total heading change of 118°, the turn through 112° is accomplished during the first 20 sec of flight. The evader accelerates continuously from Mach 0.9 to Mach 1.24, turns right through 62°, reducing its bank control from 0.86 at start to near zero at termination. The distance traversed by the two aircraft is approximately the same at C, which is the point nearest to the pursuer on the locus. The reachability condition is just met at B, so that B is a point on a Barrier section with $M_{p_o} = 1.2$, $M_{e_o} = 0.9$, $\beta_o = 180°$. The pursuer banks fully for 10 sec, slowing down to Mach 1.06 (figs. 12(d) and 13(a)) before accelerating once again. Its turn angle is 145° (fig. 13(b)). At this initial separation, the lateral distance between the pursuer and evader is sufficiently large to permit the evader to continue almost along its initial heading and accelerate. The pursuer is forced to turn around and then give chase. The terminal Mach numbers of the aircraft are very nearly the same. Beyond B, the evader escapes by simply flying straight ahead, accelerating all the time. Since both aircraft are identical, the evader will attain its maximum speed before the pursuer is able to close the gap.

The encounters starting from C_1 and C are symmetric in that the turn angles of the pursuer and evader at C_1 are almost the opposite to those at C. At C_1, the encounter terminates at a position beyond the evader's initial position (increasing y). The distance traversed by the pursuer decreases and that by the evader increases in the direction C_1CC_2. For capture in the same time, the evader must, therefore, start closer to the pursuer and the points on the segment C_1C are in fact nearer to P. At C, the encounter terminates behind the pursuer's initial position. For capture in the same time, the points to the left of C must be farther away from P than C, which explains the kink in the isochrone at C.

From table 3, the value of β_{p_f} is seen to increase from B to D. For β_{p_f} greater than that at D, the candidate points are nonoptimal, for they fall on the wrong side of the Dispersal point D. The y-axis is the axis of symmetry and the isochrone section of figure 10 for a relative heading of $\beta_o = -180°$ is the mirror image of BCD along it. It is interesting to note from figure 13(c) that in this example, there are no starting points on the isochrone for which the initial bank control is less than half.

Isochrone sections for interception for capture times ranging from 5-60 sec are shown in figure 14. The interceptor is initially at Mach 0.9 and has the target heading toward it. The target flies in a straight line at Mach 1.0. For all the points on the sections, the interceptor uses full throttle throughout. The y-axis is the zero-bank line; for initial target positions along this line, the interceptor heads straight toward the target. The half-bank and bank-saturation loci were obtained by linking the half-bank and bank-saturation points on each section. The sections for 5-20 sec end when the reachability condition is no longer met for the given terminal conditions. Their endpoints delineate the Barrier section for $M_{I_o} = 0.9$ and $\beta_o = 180°$. The sections for 30-60 sec terminate on the opposite side of the Barrier, so that there is a discontinuity in the value across the Barrier section. Two interceptor trajectories from initial points just separated by the Barrier section are shown in figure 15. The shorter trajectory involves a turn through 137° and deceleration to Mach 0.87 in 15 sec of flight. The longer trajectory requires a near 180° turn and acceleration to Mach 1.01 in 40 sec.

DISCUSSION

In the above, a method of constructing the feedback solution for pursuit-evasion and interception has been described. From the ETMs of the two vehicles, points on the isochrone (constant minimum-time loci) are obtained. Typically, each isochrone section drawn has a Dispersal point, a point where the controls assume specified levels, and Barrier points marked on it. Drawing several isochrones and linking the Dispersal points, control-level points, and points on the Barrier give sections of the corresponding surfaces. The construction of an isochrone section is demonstrated for pursuit-evasion and a section of the feedback solution is shown for interception.

In contrast to the isochrone section for pursuit-evasion, zero-bank points also appear on the section for interception. A target coming head-on without taking any evasive action can be captured in minimum time by heading straight toward it at full throttle. An active evader approaching head-on will try to turn around and flee. The pursuer turns to match the evader's anticipated final heading and accelerates to close in. Again, because the target to be intercepted does not vary its speed, a larger portion of the interceptor's ETM is globally optimal. Also, once the control-level surface sections are plotted for one value of β_o, they can be mapped for other values by rotation through the difference in β_o. The major computational effort required is in the generation of the vehicles' ETMs. Once these are available, the computation of points on the isochrone requires coordinate transformation plus a one-parameter search for pursuit-evasion, both of which require relatively little computational effort.

The ETMs for a given airplane are the same in any encounter in which that airplane participates. This makes the ETM an attractive tool for analyzing these encounters. Suboptimal approximations to the extremals on an ETM can be evaluated by comparing the approximate isochrone sections against those constructed exactly.

CONCLUSIONS

A geometric method of mapping the feedback solution by drawing isochrone sections was presented. The method is applied to pursuit-evasion and interception. For pursuit-evasion, it requires a one-dimensional search of the evader's ETM to match the initial relative heading to the specified value. In interception, the target's motion is known a priori and the additional search is avoided. In both cases, points on the Barrier and Dispersal surfaces and points on the control-level surfaces are located. The method permits the evaluation of suboptimal approximations by comparing approximate isochrone sections against the exact sections. Currently efforts are under way to extend this analysis to three dimensions through use of the energy-state approximation.

REFERENCES

1. Anderson, G. M.: A Near Optimal Closed Loop Solution Method for Non-Singular Zero-Sum Differential Games. JOTA, vol. 13, no. 3, 1974.

2. Jarmark, B. S. A.: Near-Optimal Closed Loop Strategy for Aerial Combat Games. TRITA-REG-7602, Dept. of Automatic Control, The Royal Institute of Technology, Stockholm, Sweden, Mar. 1976.

3. Isaacs, R.: Differential Games. John Wiley & Sons, New York, 1965.

4. Well, K. H.; Faber, B.; and Berger, E.: Optimization of Tactical Aircraft Maneuvers Utilizing High Angles of Attack. AIAA J. Guidance Control, vol. 5, no. 2, Mar.-Apr. 1982, pp. 131-137.

5. Calise, A. J.: Singular Perturbation Techniques for On-Line Optimal Flight Path Control. AIAA Paper 79-1621, Boulder, Colo., 1979.

6. Shinar, J.: Validation of Zero-Order Feedback Strategies for Medium-Range Air-to-Air Interception in a Horizontal Plane. NASA TM-84237, 1982.

7. Farber, N.; and Shinar, J.: An Approximate Feedback Solution of a Variable Speed Nonlinear Pursuit-Evasion Game between Two Airplanes in a Horizontal Plane. AIAA Paper 80-1597, Danvers, Mass., 1980, pp. 337-347.

8. Kelley, H. J.: Aircraft Maneuver Optimization by Reduced Order Approximations. Advances in Control and Dynamic Systems, vol. 10, Academic Press, 1973.

9. Parsons, M. G.: Three-Dimensional, Minimum Time Turns to a Point and onto a Line for a Supersonic Aircraft with a Constraint on Maximum Velocity. Ph.D. Dissertation, Stanford U., Stanford, Calif., Aug. 1972.

10. Rajan, N.; Prasad, U. R.; and Rao, N. J.: Pursuit-Evasion of Two Aircraft in a Horizontal Plane. AIAA J. Guidance Control, vol. 3, no. 3, May-June 1980, pp. 261-267.

11. Prasad, U. R.; Rajan, N.; and Rao, N. J.: Planar Pursuit-Evasion with Variable Speeds. Part 1: Extremal Trajectory Maps. JOTA, vol. 33, no. 3, Mar. 1981, pp. 401-418.

12. Rajan, N.; Prasad, U. R.; and Rao, N. J.: Planar Pursuit-Evasion with Variable Speeds. Part 2: Barrier Sections. JOTA, vol. 33, no. 3, Mar. 1981, pp. 419-432.

13. Rajan, N.: Differential Game Analysis of Two Aircraft Pursuit-Evasion. Ph.D. Dissertation, School of Automation, Indian Institute of Science, Bangalore, July 1978.

14. Rajan, N.; and Ardema, M. D.: Barrier and Dispersal Surfaces in Minimum Time Interception. NASA TM-84241, May 1982.

TABLE 1.- TERMINAL HEADING FOR THE EXTREMALS COMPRISING FIGURE 7

τ_f, sec	β_f ($\|\omega\|$ = 0.5), deg	β_f ($\|\omega\|$ = 1), deg
5	1.62	3.49
10	.33	.83
15	.09167	.206
20	.03	.065
30	.00487	.00917
40	.00096	.00176
50	.00024	.00042
60	.000065	.000114

TABLE 2.- FULL-BANK, FULL-THROTTLE ARCS

τ_f, sec	$\Delta\beta$, deg	ΔM	R, km
5	58.12	-0.052	1.32
10	112.94	-.08	2.28
15	165.74	-.096	2.72
20	217.4	-.105	2.62

TABLE 3.- TERMINAL-VELOCITY-VECTOR VALUES
[Relating to fig. 10]

Point	β_{pf} ($\times 10^{-3}$)	M_{pf}	β_{ef} ($\times 10^{-3}$)	M_{ef}
D	-0.7	1.377	1.06	1.184
C_1	-1.1	1.343	.68	1.205
C	-1.8	1.285	.38	1.24
C_2	-2.2	1.263	.26	1.251
B	-2.3	1.259	.23	1.252

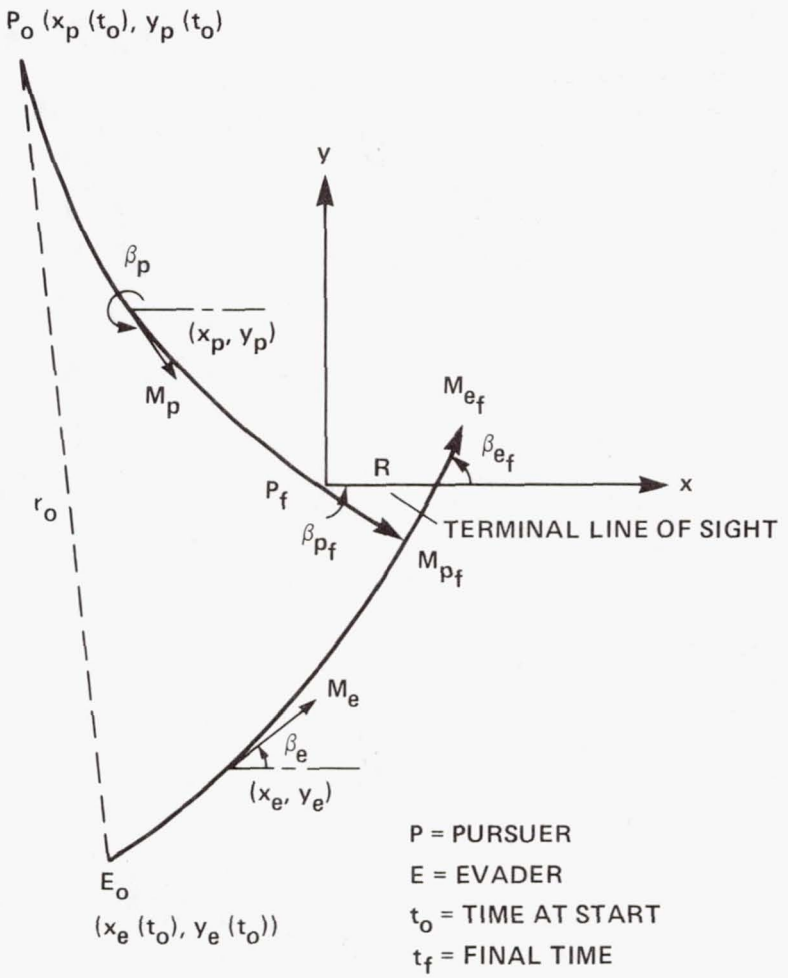

Figure 1.- The coordinate system.

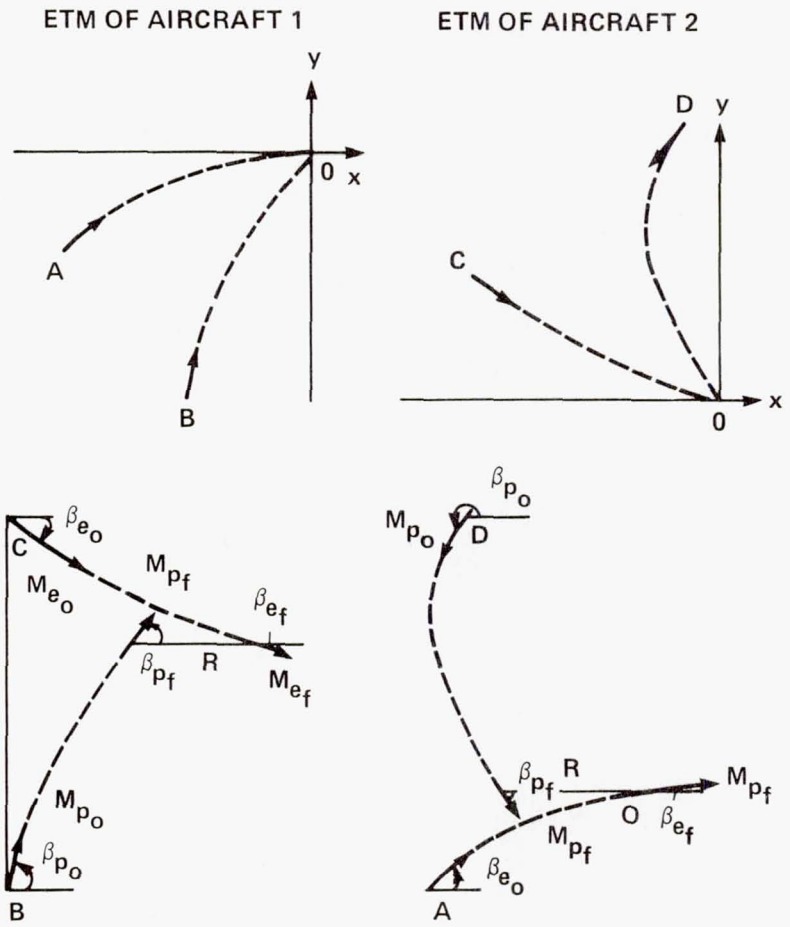

Figure 2.- Piecing encounters from ETMs.

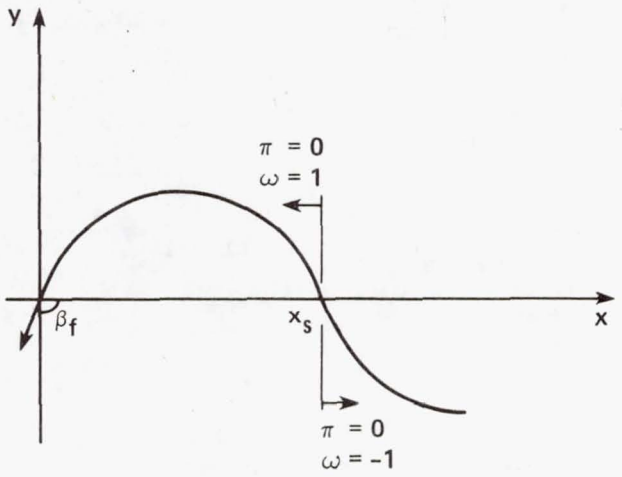

(a) Switch in ω.

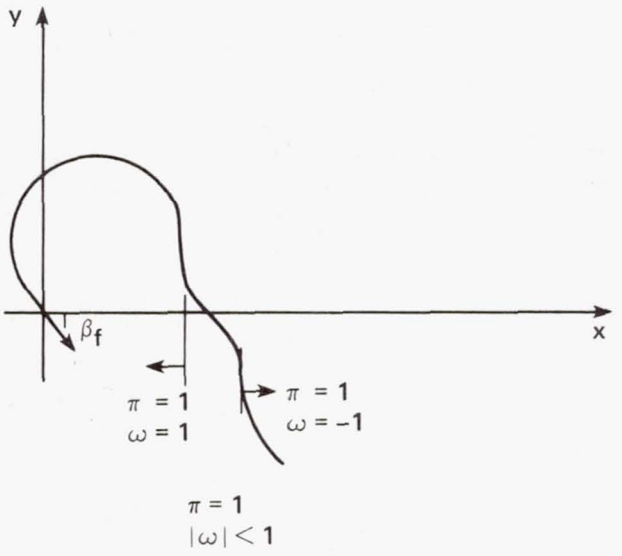

(b) Gradual change in ω.

Figure 3.- Changes in ω as the extremal crosses the x-axis.

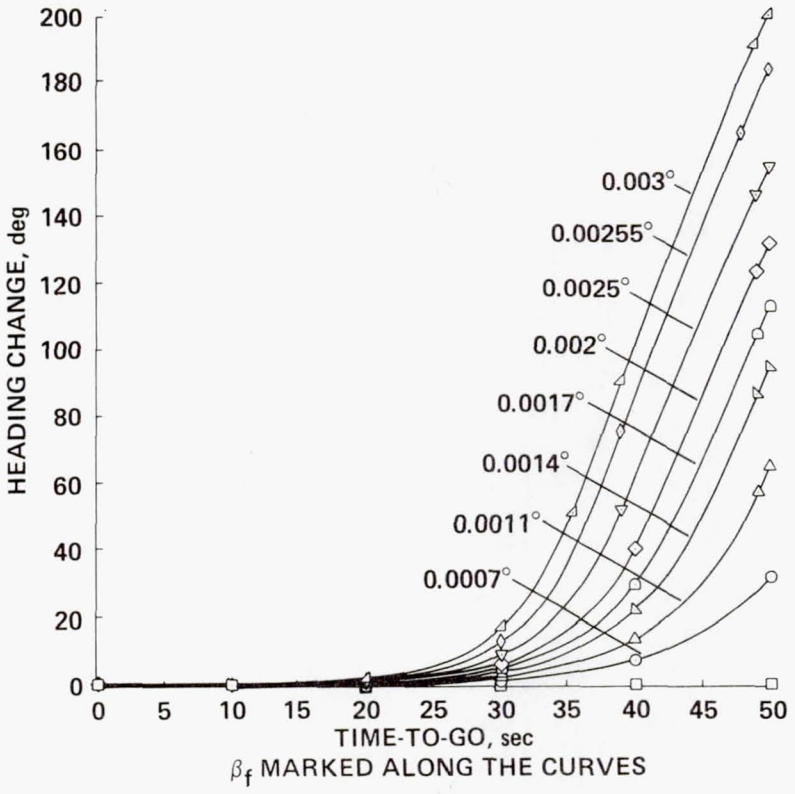

(a) Heading time-history.

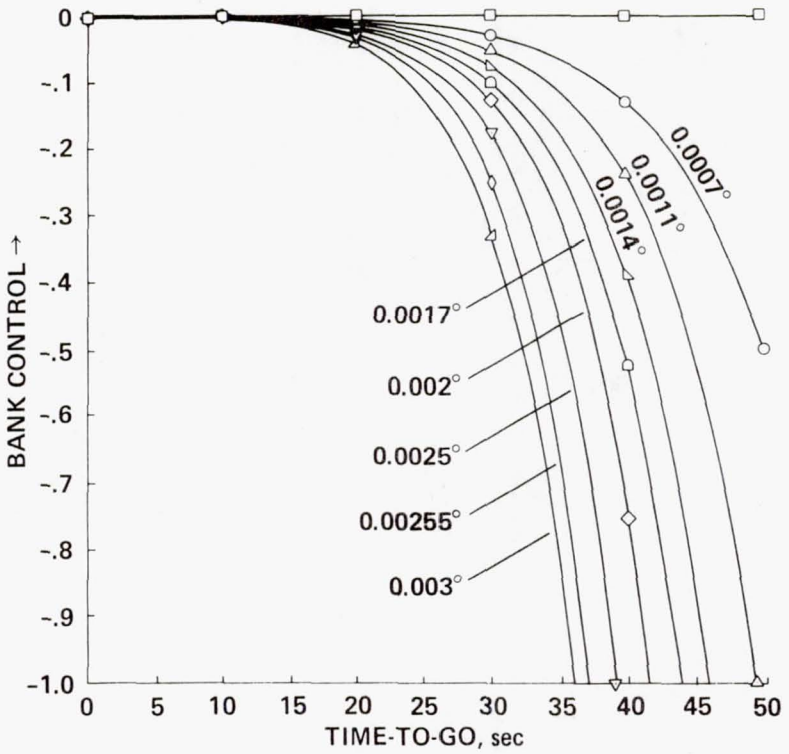

(b) Bank-control time-history.

Figure 4.- An extremal trajectory map.

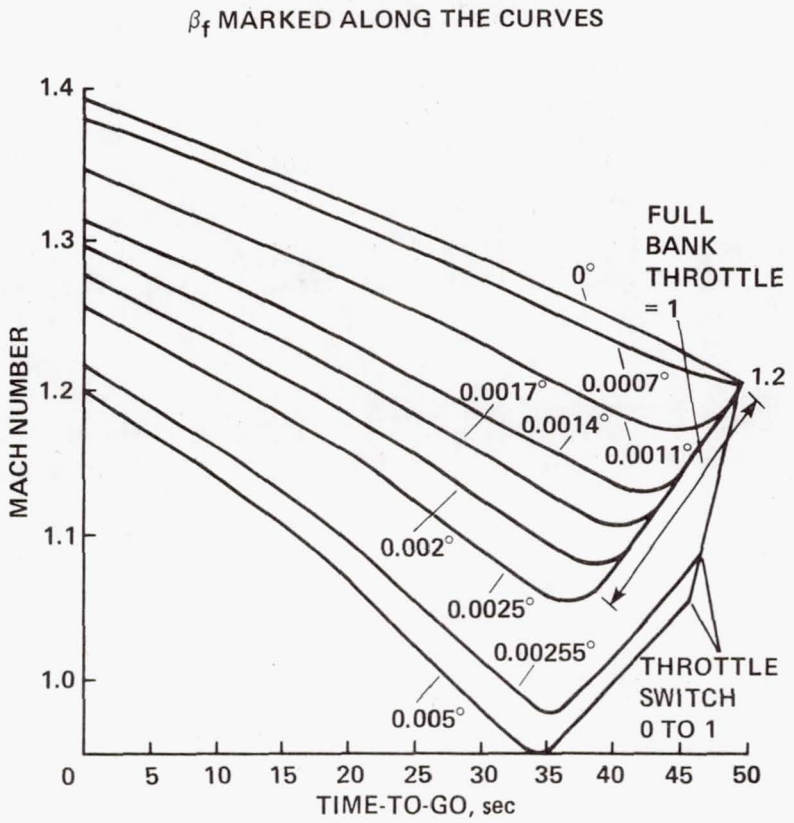

(c) Mach number time-history.

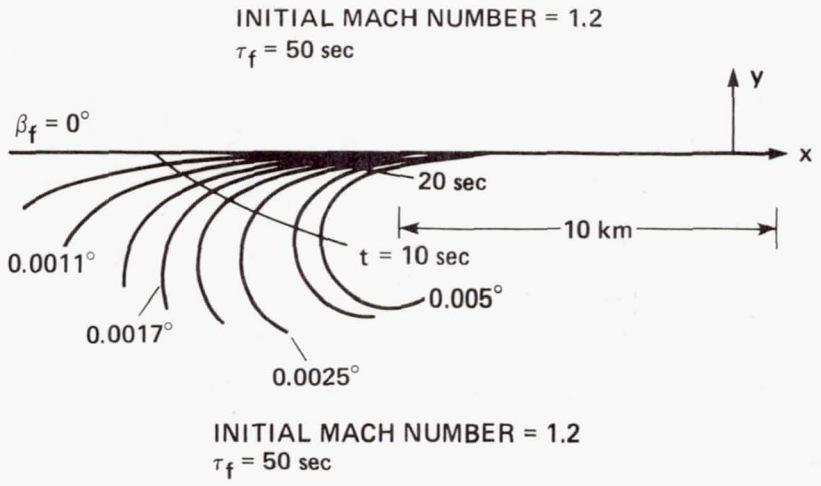

(d) Trajectories in the plane.

Figure 4.- Concluded.

INITIAL MACH NUMBER = 0.9

No.	β_f	τ_f	$\Delta\beta$	ΔM
1	0.001°	50	142°	0.052
2	0.6°	20	136°	0.052
3	0.7°	20	142°	0.043

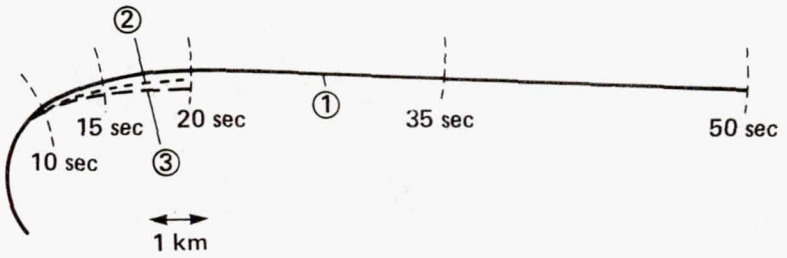

Figure 5.- Comparison of extremals of different duration.

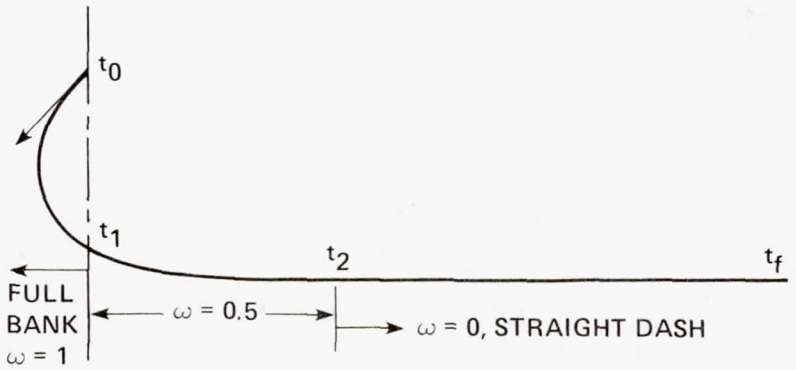

THROTTLE SETTING = 1

Figure 6.- A possible suboptimal trajectory.

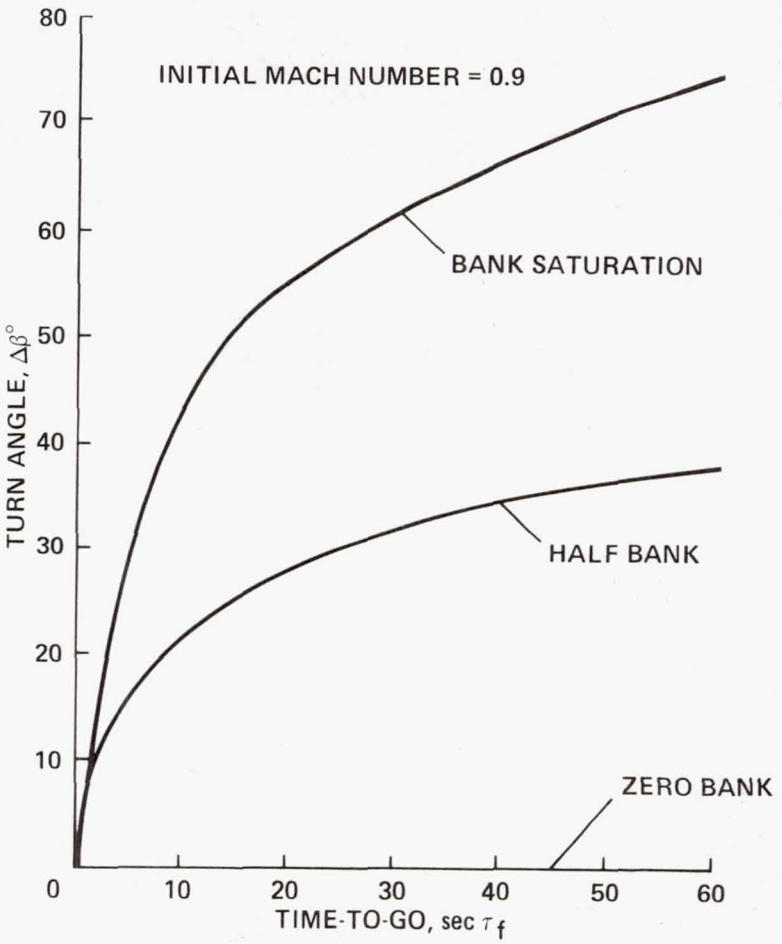

(a) Turn angle.

Figure 7.- Characteristics of extremals as a function of time-to-capture.

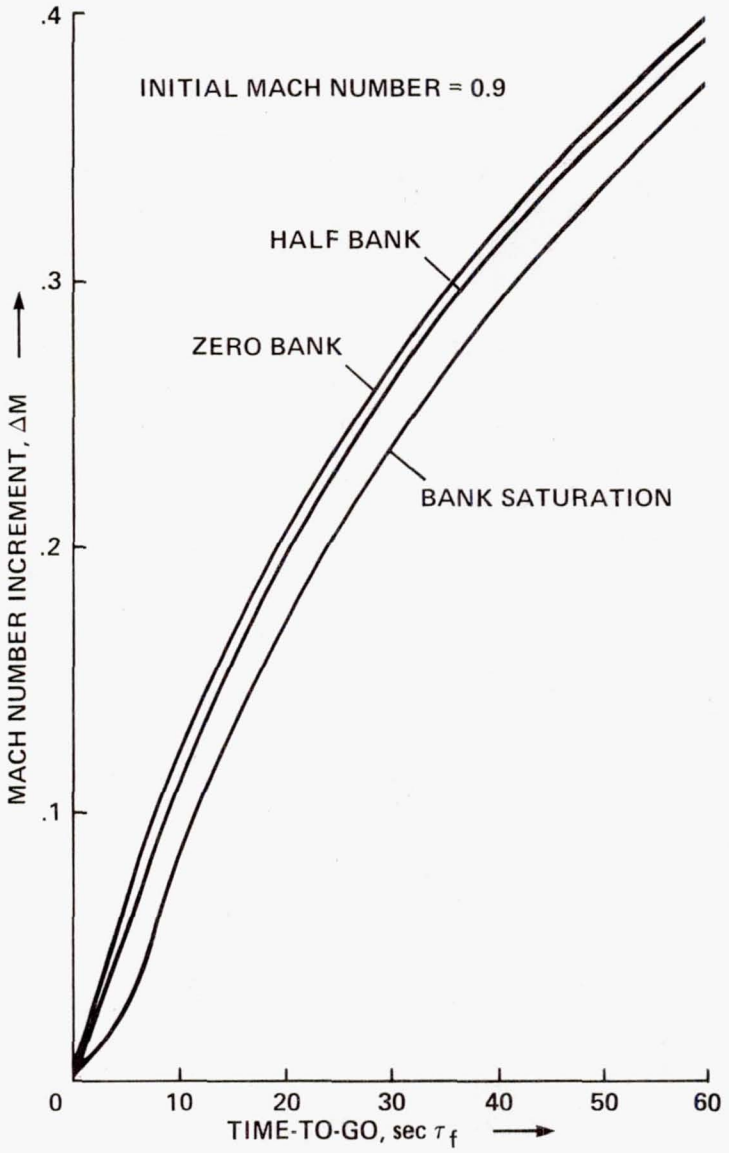

(b) Mach number increment.

Figure 7.- Continued.

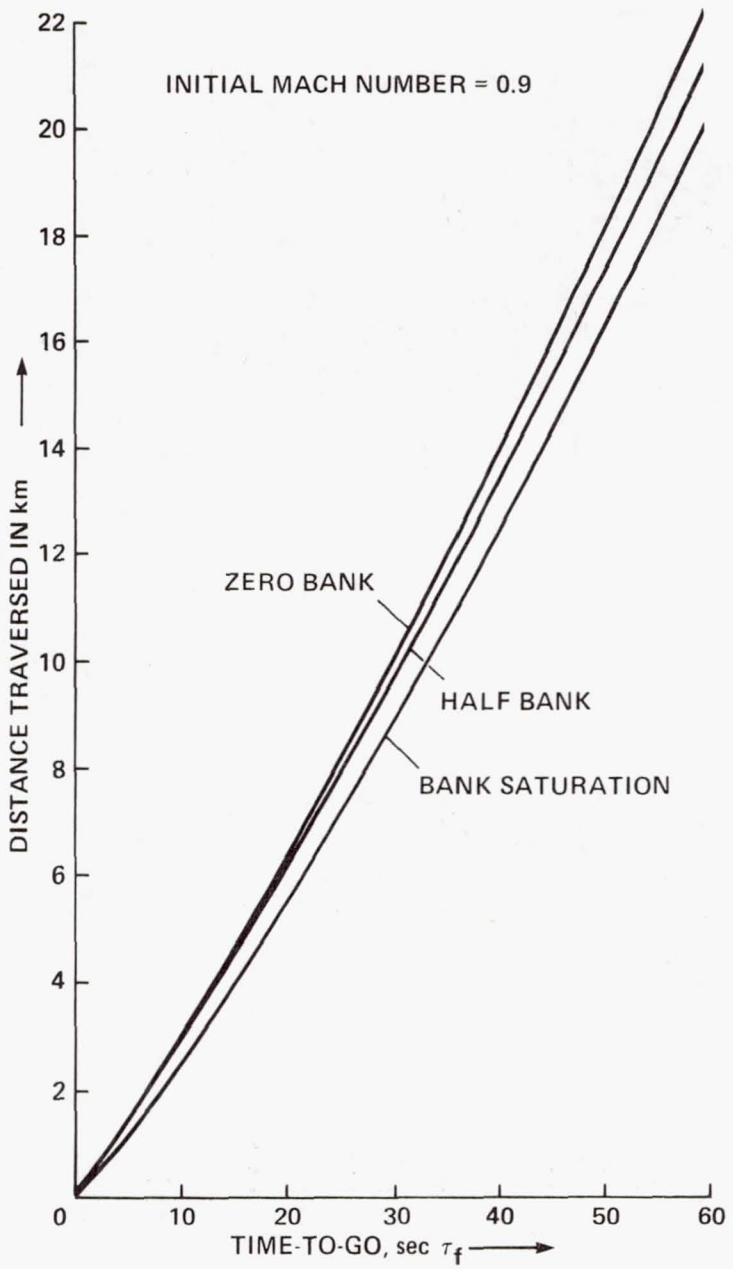

(c) Distance traversed.

Figure 7.- Concluded.

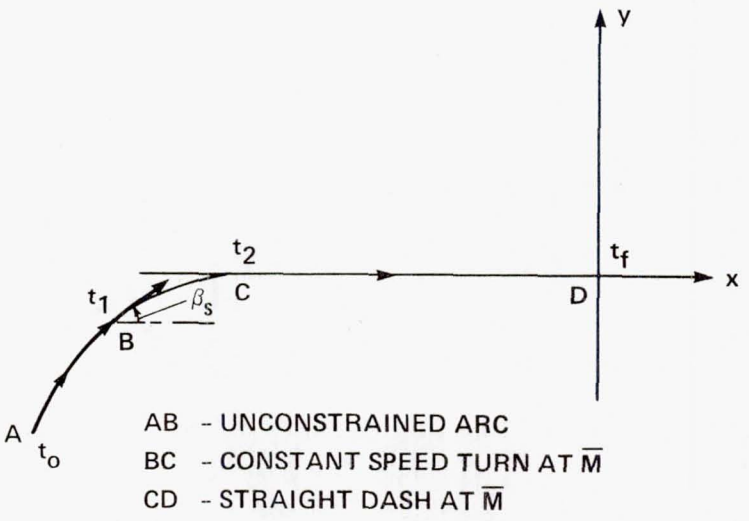

(a) Schematic.

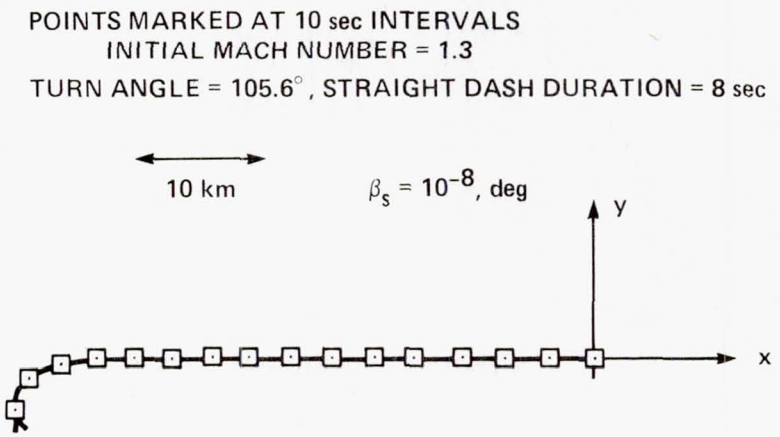

(b) An example extremal lasting 150 sec.

Figure 8.- An extremal with a cruise arc.

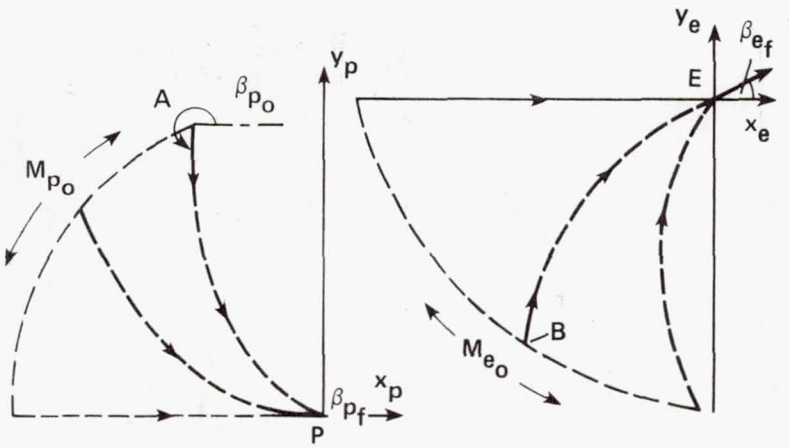

(a) PURSUER'S ETM (b) EVADER'S ETM

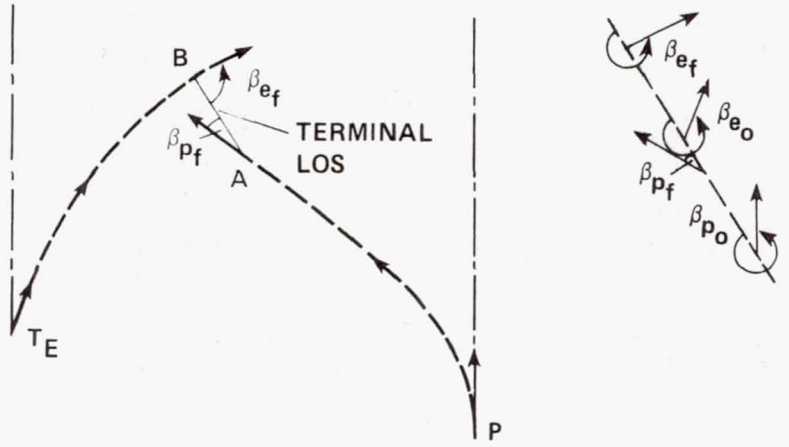

(c) POINT ON THE LOCUS

Figure 9.- Construction of a point on an isochrone.

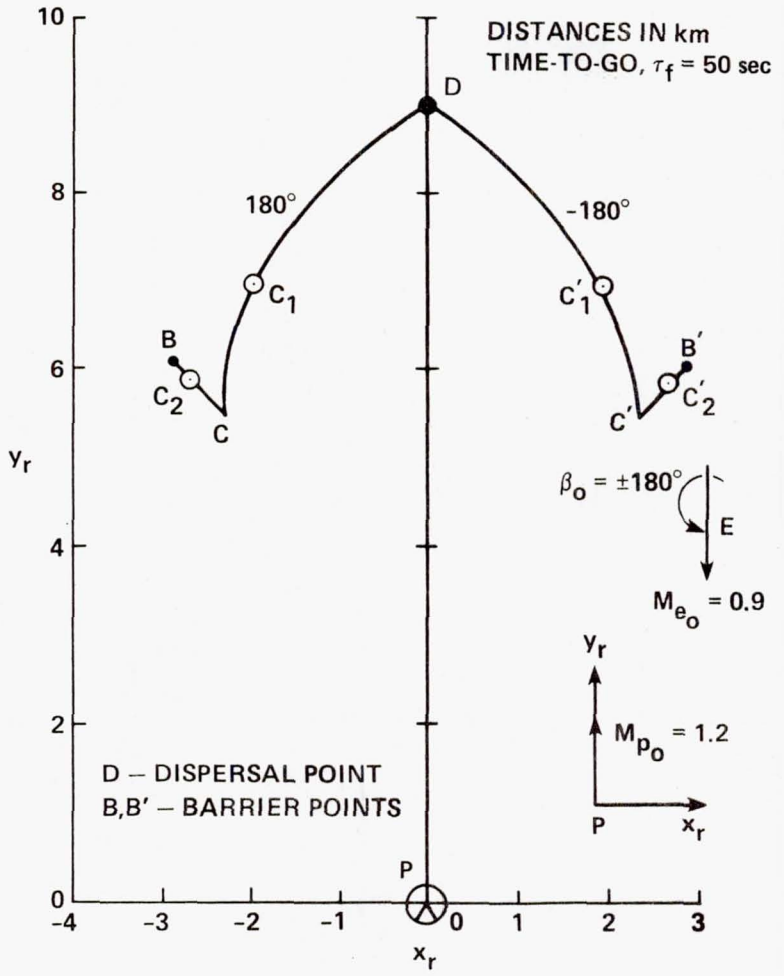

Figure 10.- An isochrone section for pursuit-evasion.

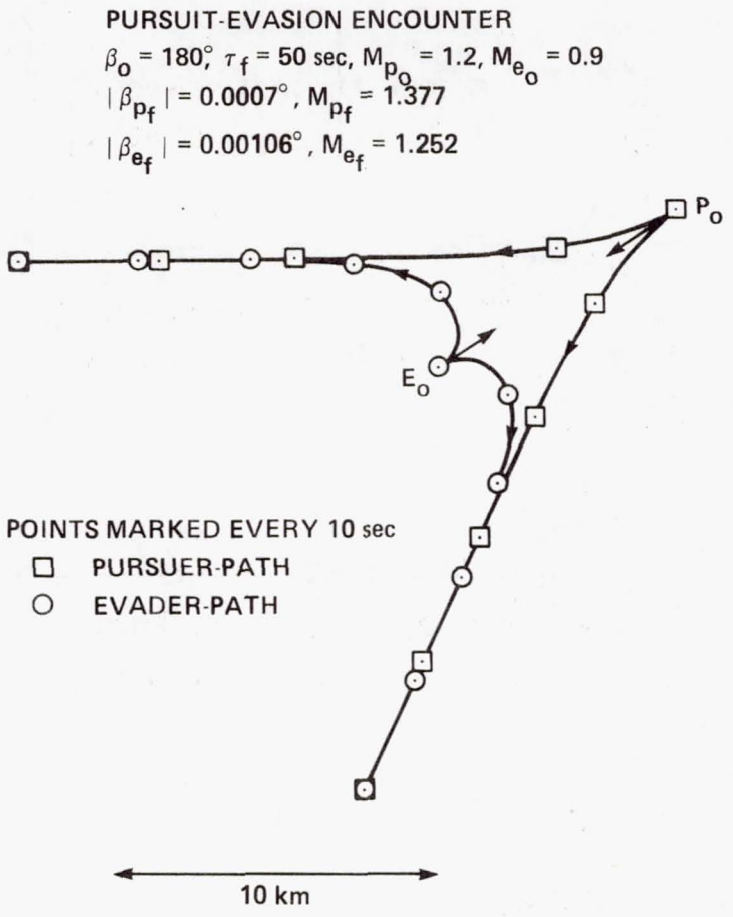

Figure 11.- Two encounters starting from Dispersal point D.

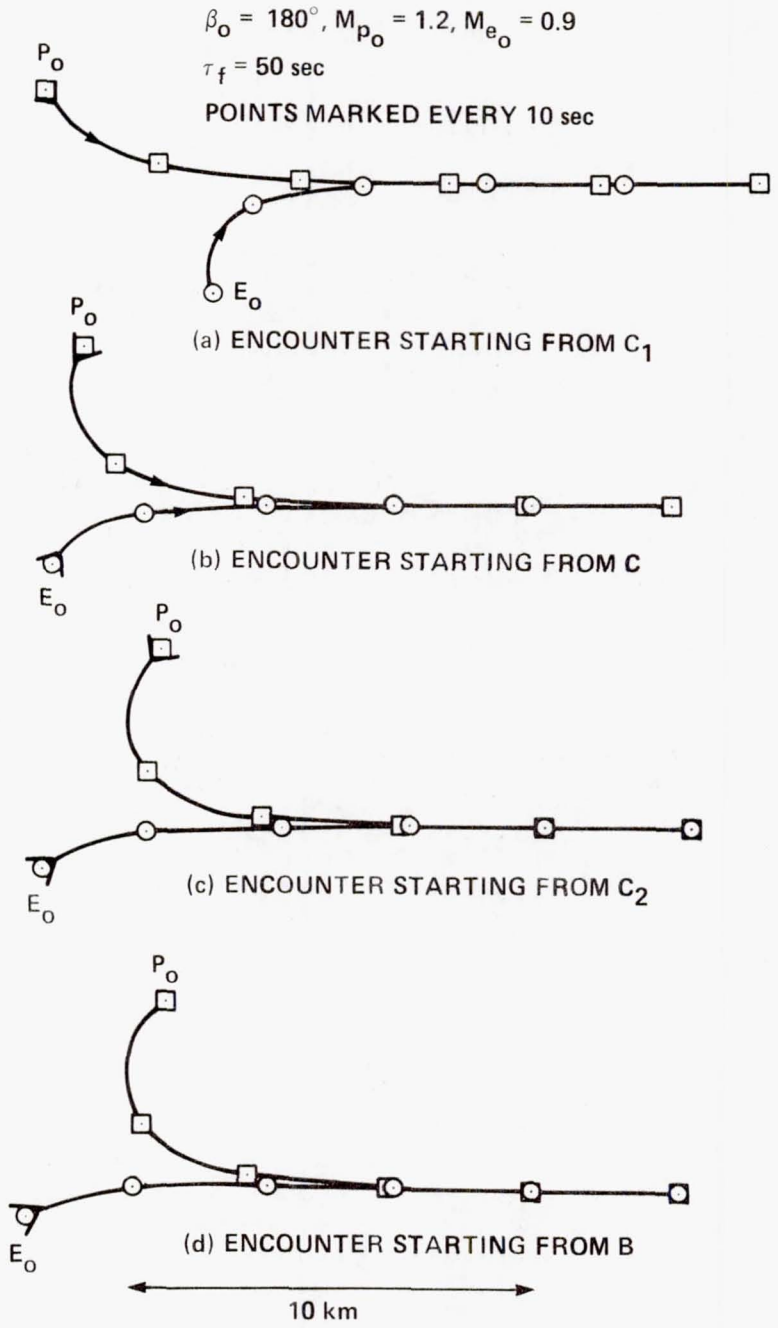

Figure 12.- Pursuit-evasion encounters.

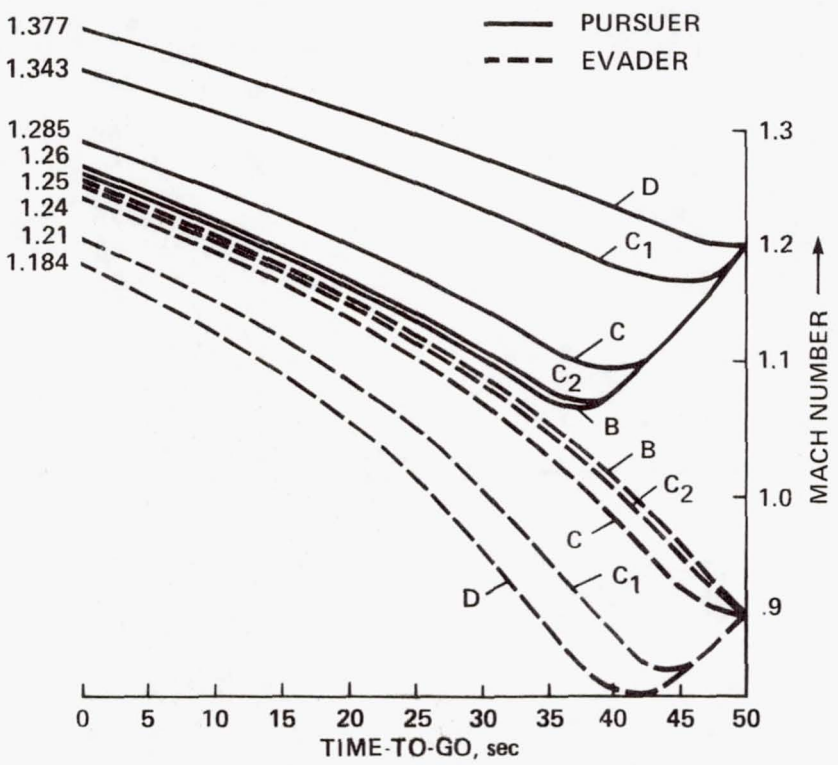

(a) Mach number.

Figure 13.- Time-histories for pursuer and evader.

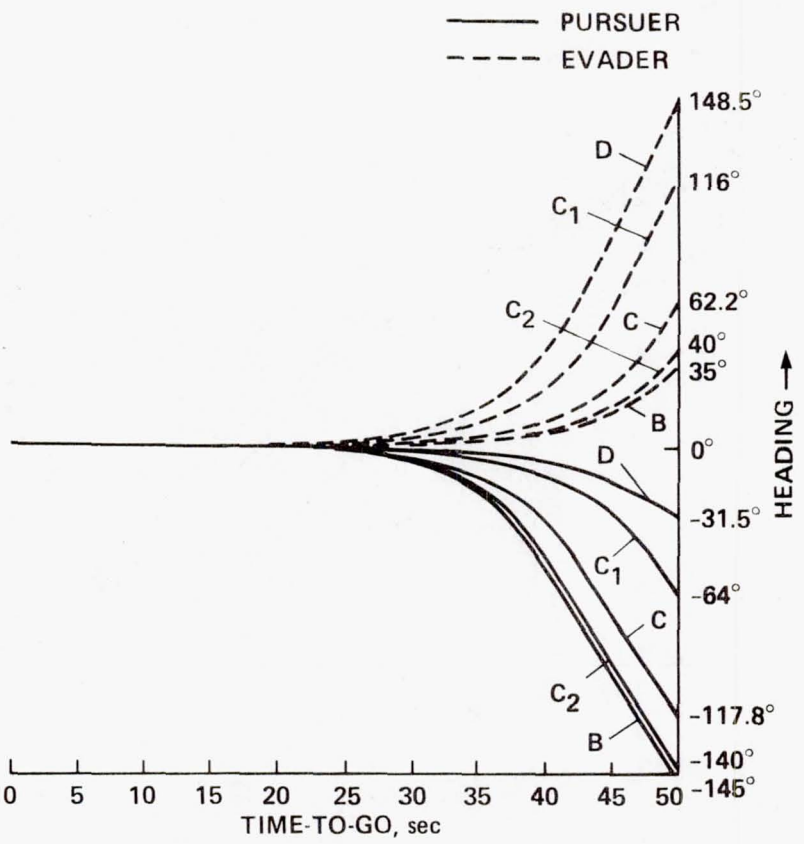

(b) Heading.

Figure 13.- Continued.

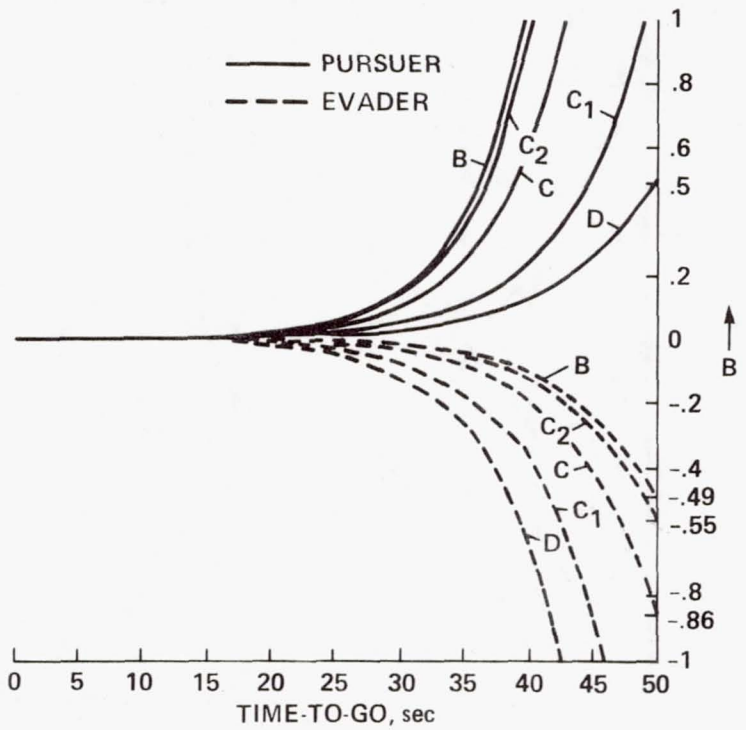

(c) Bank control.

Figure 13.- Concluded.

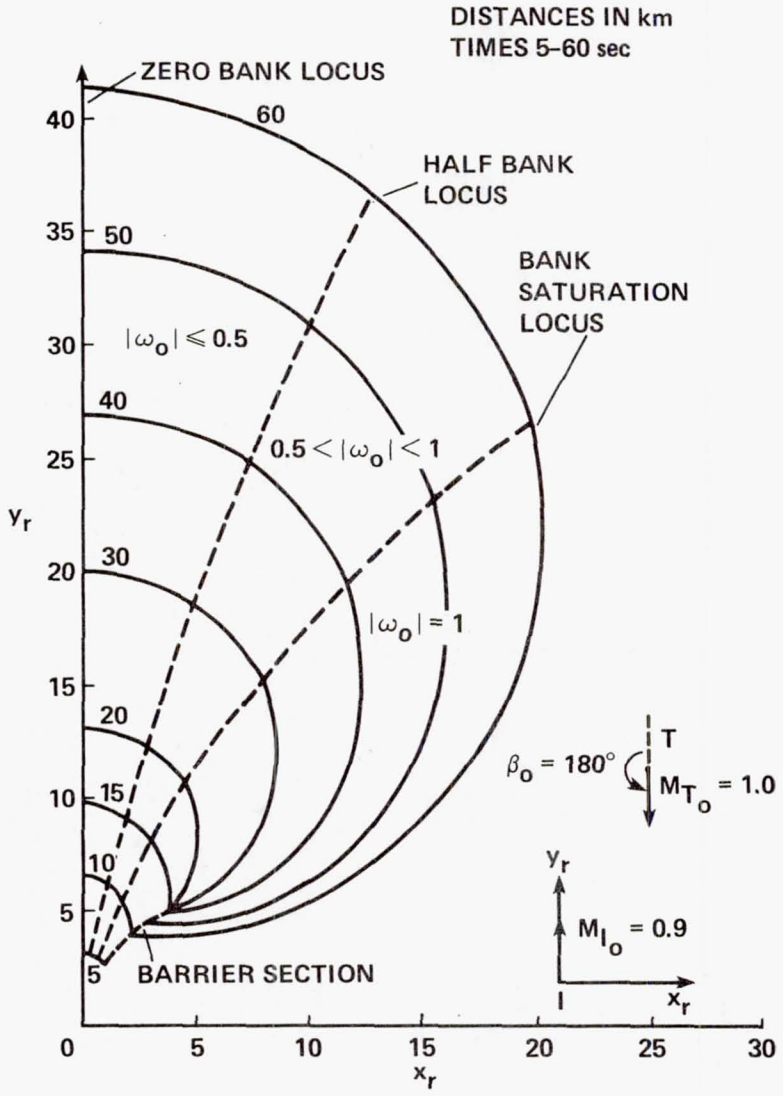

Figure 14.- Feedback section for interception.

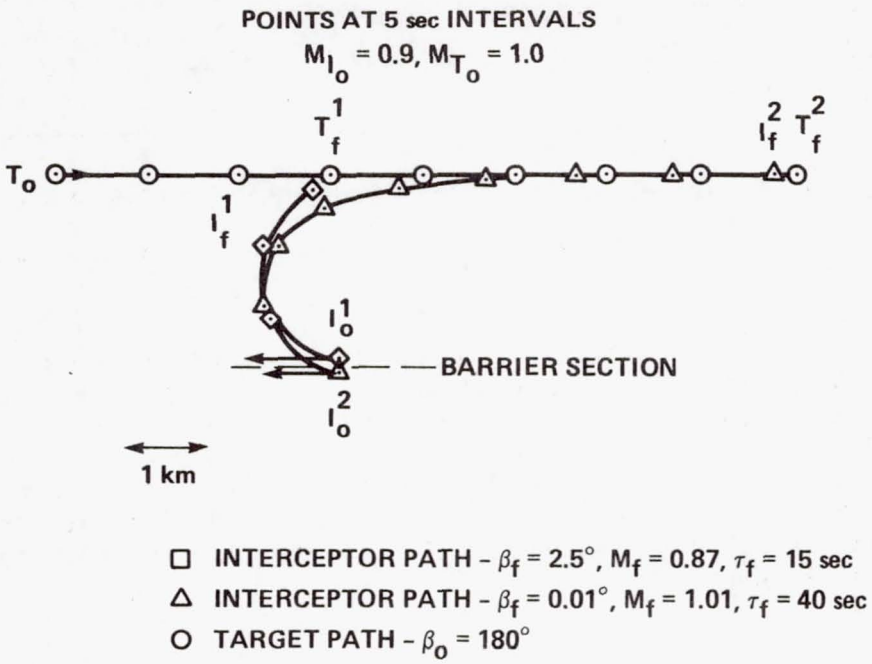

Figure 15.- Interception encounters in the plane.

1. Report No.	2. Government Accession No.	3. Recipient's Catalog No.
NASA TM 84311		

4. Title and Subtitle	5. Report Date
OPTIMAL FEEDBACK STRATEGIES FOR PURSUIT-EVASION AND INTERCEPTION IN A PLANE	February 1983
	6. Performing Organization Code
7. Author(s)	8. Performing Organization Report No.
N. Rajan* and M. D. Ardema	A-9177
	10. Work Unit No.
9. Performing Organization Name and Address	T-3309
NASA Ames Research Center Moffett Field, Calif. 94035	11. Contract or Grant No.
	13. Type of Report and Period Covered
12. Sponsoring Agency Name and Address	Technical Memorandum
National Aeronautics and Space Administration Washington, D.C. 20546	14. Sponsoring Agency Code 505-34-11

15. Supplementary Notes

Point of Contact: N. Rajan, Ames Research Center, M/S 210-9, Moffett Field, Calif. 94035. (415) 965-5431 or FTS 448-5431.

16. Abstract

Variable-speed pursuit-evasion and interception for two aircraft moving in a horizontal plane are analyzed in terms of a coordinate frame fixed in the plane at termination. Each participant's optimal motion can be represented by extremal trajectory maps. These maps are used to discuss suboptimal approximations that are independent of the other participant. A method of constructing sections of the Barrier, Dispersal, and control-level surfaces and thus determining feedback strategies is described. Some examples are shown for pursuit-evasion and the minimum-time interception of a straight-flying target.

17. Key Words (Suggested by Author(s))	18. Distribution Statement
Pursuit-evasion Minimum-time interception Aircraft flightpath optimization	Unlimited Subject Category - 08

19. Security Classif. (of this report)	20. Security Classif. (of this page)	21. No. of Pages	22. Price*
Unclassified	Unclassified	34	A03

*For sale by the National Technical Information Service, Springfield, Virginia 22161